Supporting Information

Directed Self-Assembly of Micron-Sized Gold Nanoplatelets into Oriented Flexible Stacks with Tunable Interplate Distance

Hanumantha Rao Vutukuri[§*], Stéphane Badaire[§], D. A. Matthijs de Winter[+], Arnout Imhof[§], Alfons van Blaaderen[§*]

[§] Soft Condensed Matter, Debye Institute for Nanomaterials Science, Utrecht University, Princetonplein1, 3584 CC, Utrecht, The Netherlands

[+] Department of Biology, Utrecht University, Padualaan 8, 3584 CH, Utrecht, The Netherlands.

Corresponding Authors

* (H.R.V) E-mail: H.R.Vutukuri@uu.nl

*(A.v.B) E-mail: A.vanBlaaderen@uu.nl

Supplementary movie captions:

Movie S1: This movie shows Brownian motion of flexible 1D stacks of gold nanoplatelets at 0.8 mM KCl. The movie was acquired at 10 fps and it is played at 20 fps.

Movie S2: This movie illustrates the formation of bands consisting of stacks of particles at a concentration of 0.8 mM KCl, an applied electric field strength of $E_{rms} \approx 0.07$ Vμm^{-1}, and a frequency of $f = 200$ kHz. Smaller columns and/or individual particles are the result of circulations. When the field is turned off, the particles reassembled into stacks instantaneously. Subsequently, the reformed stacks are directed to ordered structures using a low electric field

($E_{rms} \approx 0.015$ Vμm^{-1}, $f = 200$ kHz), which is below the critical field strength for the onset of instabilities. The movie was acquired at 10 fps and it is played at 24 fps.

Supplementary Figures

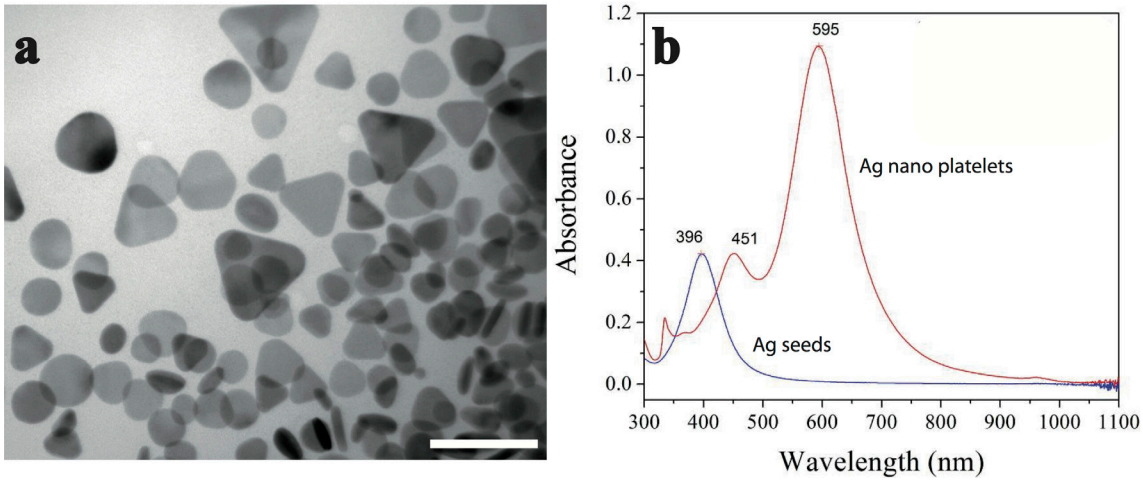

Figure S1. (a) TEM image of Ag nano platelets were prepared by illumination of Ag seeds with the tube lights. (b) UV-vis-NIR spectra of dispersions of Ag seeds, and Ag nano platelets in water, respectively. Scale bar is 100 nm.

EDX-STEM mapping:

The EDX maps were acquired using an EDAX SiLi detector at 200 kV acceleration voltage with a screen current of 200 pA in STEM mode. Tecnai Imaging and Analysis software (TIA) was used for acquisition of the data as well as for drift correction. A map of 740 X 740 nm^2 was acquired with a pixel resolution of 45 X 45 pixel^2, which gives a pixel size of 16 X 16 nm^2. The dwell time per pixel was 7.5 seconds, which resulted in a total mapping time of about 4.5 hours.

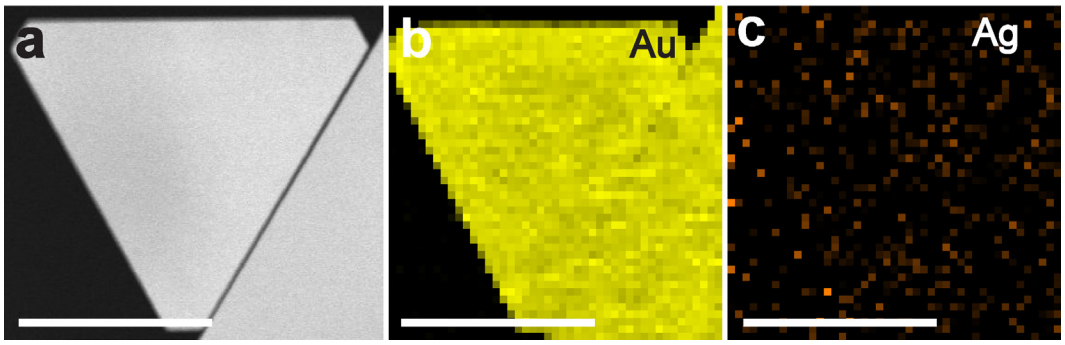

Figure S2. EDX-STEM mapping. (a) STEM image of a gold platelet. (b-c) The corresponding elemental mapping of the Au, and Ag elements, respectively. Scale bars are 500 nm.

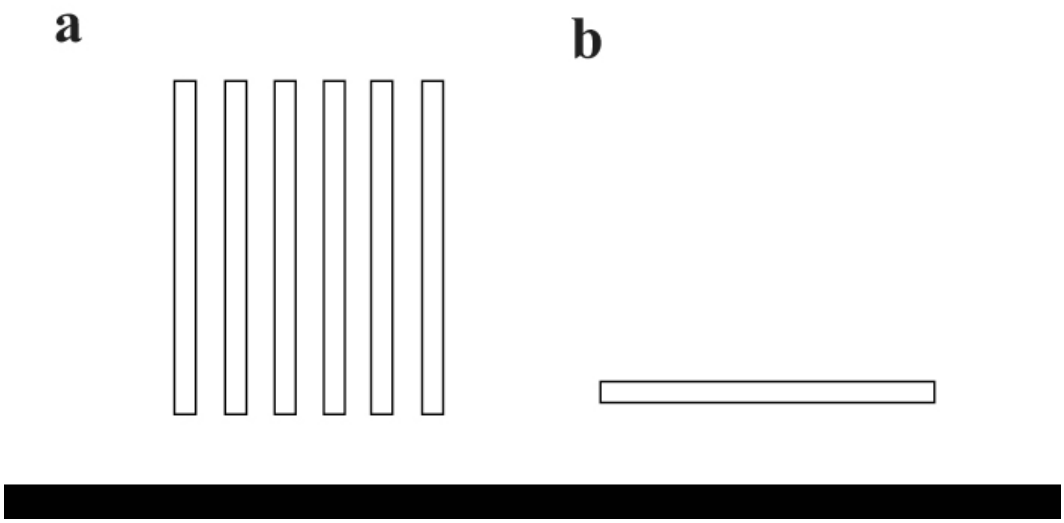

Figure S3. Illustration of interaction potential between the particles. State (a) a gold particle interacts with an other one and joins the stack. State (b) a particle does not interact and lays down on the surface.

Particle interactions

The stability of many charge stabilized colloidal dispersions can be described in terms of a screened electrostatic repulsive potential and an attractive van der Waals potential between the particles using the DLVO (Deryaguin-Landau-Verwey-Overbeek) theory. [1-4] For semi-infinite

plates of area *S*, separated by a distance *d*, and assumed to be at constant surface potential Ψ_o (-35 mV); the repulsive potential can be approximated as

$$\frac{V_R}{S} = \frac{64\, n\, K_B\, T}{\kappa}\, \gamma^2\, exp(-\kappa d) \qquad (1)$$

where

$$\gamma = \frac{exp\left(\frac{e\psi_o}{2K_BT}\right) - 1}{exp\left(\frac{e\psi_o}{2K_BT}\right) + 1}$$

where d is the distance between the platelets, n is the ion concentration, K_B is Boltzman's constant, T the absolute temperature, e is the elementary charge, and κ is the inverse Debye screening length. The Debye screening length κ^{-1} is a measure for the range of electrostatic repulsion that depends on the ion concentration (assumed to be monovalent), n, according to

$$\kappa^{-1} = n^{-\frac{1}{2}} \left(\frac{e^2}{\varepsilon\, \varepsilon_o K_B T}\right)^{-\frac{1}{2}} \qquad (2)$$

The van der Waals attractive potential between two half spaces is given by

$$\frac{V_A}{S} = \frac{H_{eff}\,(d)}{12\pi\ d^2} \qquad (3)$$

where the Hamaker function H_{eff} is estimated by the Lifshitz theory.

$$H_{eff}(d) = -\frac{3}{2}\, K_B\, T \sum_{n=0}^{\infty}{}' \int_{r_n}^{\infty} x \left\{ln\left[1 - \Delta_{pm}^2\, e^{-x}\right] + ln\left[1 - \bar{\Delta}_{pm}^2\, e^{-x}\right]\right\} dx$$

where $\Delta_{jk} = (\varepsilon_j\, s_k - \varepsilon_k\, s_j) / (\varepsilon_j\, s_k + \varepsilon_k\, s_j)$, $\bar{\Delta}_{jk} = (s_k - s_j) / (s_k + s_j)$, and p, m, denote the particle and medium respectively,

$s_k^2 = x^2 + (2\, \xi_n d\, c^{-1})^2\, (\varepsilon_k - \varepsilon_m)$,

$r_n = \left(2\, d\, \xi_n \sqrt{\varepsilon_m}\right)/c$, $\xi_n = (2\pi n\, K_B T)/h$, $\varepsilon_k = \varepsilon_k(i\, \xi_n)$, here $i = \sqrt{-1}$, h is Planck's constant, c is the speed of light in vacuum, and $\varepsilon_k(\omega)$ is dielectric constant of material k at the frequency ω. The prime ($'$) next to the summation indicates that the first term (n=0) is multiplied by (1/2). The factor of 1/2 avoids double counting, while the remainder of this factor accounts for the screening of the zero frequency contribution. Note that the physical properties of the materials enter through the function $\varepsilon_k(i\, \xi_n)$. In our calculations we used the optical properties of gold and water from the handbook of optical constants of solids. [5] The Debye screening lengths were calculated using the above mentioned *eq.* 2 for different salt concentrations.

The total interaction potential between the platelets is the sum of the screened electrostatic repulsive potential and the van der Waals attraction

$$V_{DLVO} = V_R + V_A$$

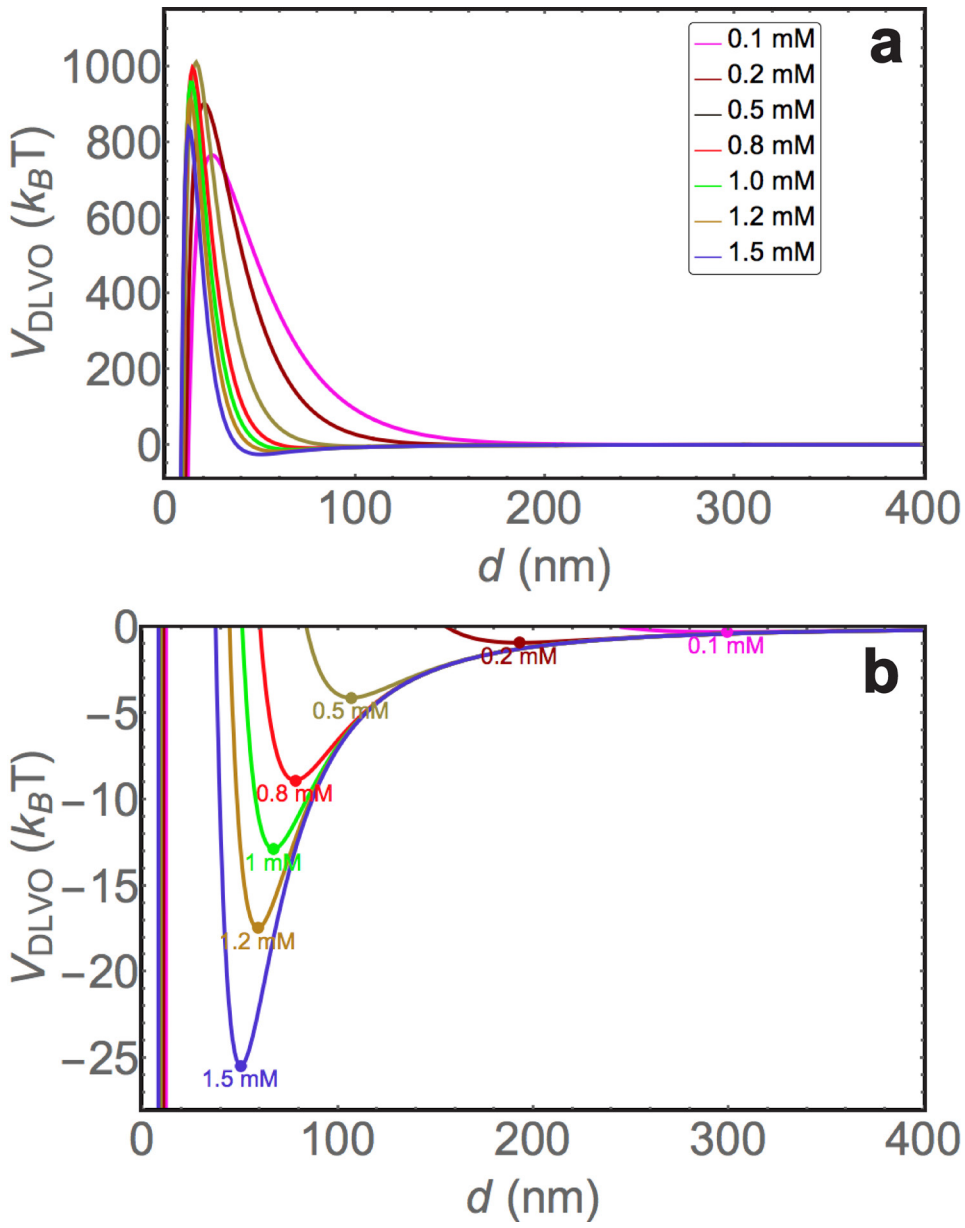

Figure S4: DLVO potential between two gold platelets of size 0.17 μm^2, surface potential of -40 mV in 30wt% glycerol solution. Interaction potentials were calculated as a function of the inter-platelet distance *d* for different salt concentrations. (a) DLVO potential. (b) The secondary minimum of the DLVO potential.

Electrohydrodynamic instability

Upon increasing the field strength (E_{rms} = 0.04 Vμm^{-1}, f = 200 kHz), the columns that were initially aligned perpendicular to the applied field direction started to rotate slowly, thereby forming bands at nearly 45^{o} relative to the applied field direction, as shown in Figure S5. The speed and direction of the rotation depends on the relative position of the columns with respect to the external electric field. Within a band, the columns were dynamically unstable, circulating in a counter-clockwise fashion, if the band tilted to the right relative to the applied field, and circulating clockwise, if the band tilted to the left. There were isolated bands, and also bands tilted in opposite directions joined together at the ends (Figure S5c-d). The speed of columns circulation increased when the strength of the applied field was increased, and the circulation was also sensitive to the frequency of the field. Although we were not able follow the dynamics on a single particles level, we did see the rotation of columns at field strength (E_{rms}= 0.07Vμm^{-1}, f = 200 kHz). After 2-3 mins the field was turned off, and it was observed that the circulations immediately stopped. Many shorter columns formed, which resulted from breakage of longer ones due to a strong rotational motion. Here, we demonstrate how the field can be exploited to grow longer columns from smaller ones (Figure S5g-h). The same dispersion was exposed to a lower field strength E_{rms} = 0.015 Vμm^{-1}, which was well below the critical field strength for the onset of the instability. The small columns then started to join together again and forming longer columns thereby moving towards the 2D columnar phase as shown in Figure S5g-h. These phenomena clearly demonstrated that the presence of the field altered the distribution of column lengths. It is not clear at present if this was simply due to changes of local concentrations of the columns (by the aligning effect of the field) or if there were also additional attractive components between the column ends and/or sides induced by the electric fields.

Since our system is complex we restricted ourselves to a more qualitative interpretation. In the following, we adapt a simple time scaling argument that is already reported in literature[6, 7] for spherical particles, bringing our observations in line with others already described in literature. It is instructive to compare two time scales: i) the time required (τ_D) for the counter-ions to diffuse over the distance of ($\delta + \kappa^{-1}$),

$$\tau_D = \frac{(\delta + 2\kappa^{-1})^2}{2D}$$

and ii) the oscillation period (τ_p) of the alternating field , where δ is the thickness of the plate, and κ^{-1} is the Debye screening length.

The counterions diffusivity (D) is on the order of 10^{-9} m^2/s, the Debye screening length is about 8 nm for a 1.50 mM suspension, the thickness of the particle δ is about 16 nm and $\tau_D \approx 10^{-6}$. Here we used a 200 kHz frequency field, and therefore an oscillation period of the applied field is $\tau_p = 1/2\pi f$. When the oscillation period of the applied field τ_p ($O(10^{-6})$) < diffusion time of the counterions $\tau_D \approx 10^{-6}$ a phase lag develops between the induced dipole moment of the double layer and the applied electric field. Due to this phase shift, the time-averaged torque on each particle is non-zero. Therefore, when the two particles are not aligned parallel or perpendicular to the direction of the applied field, they will spin. The torque has a maximum amplitude at $\theta = 45^o$, which induces a strong flow and instabilities. We believe that these circulations have electrohydrodynamic origin as was reported for the spherical particles.[6, 7]

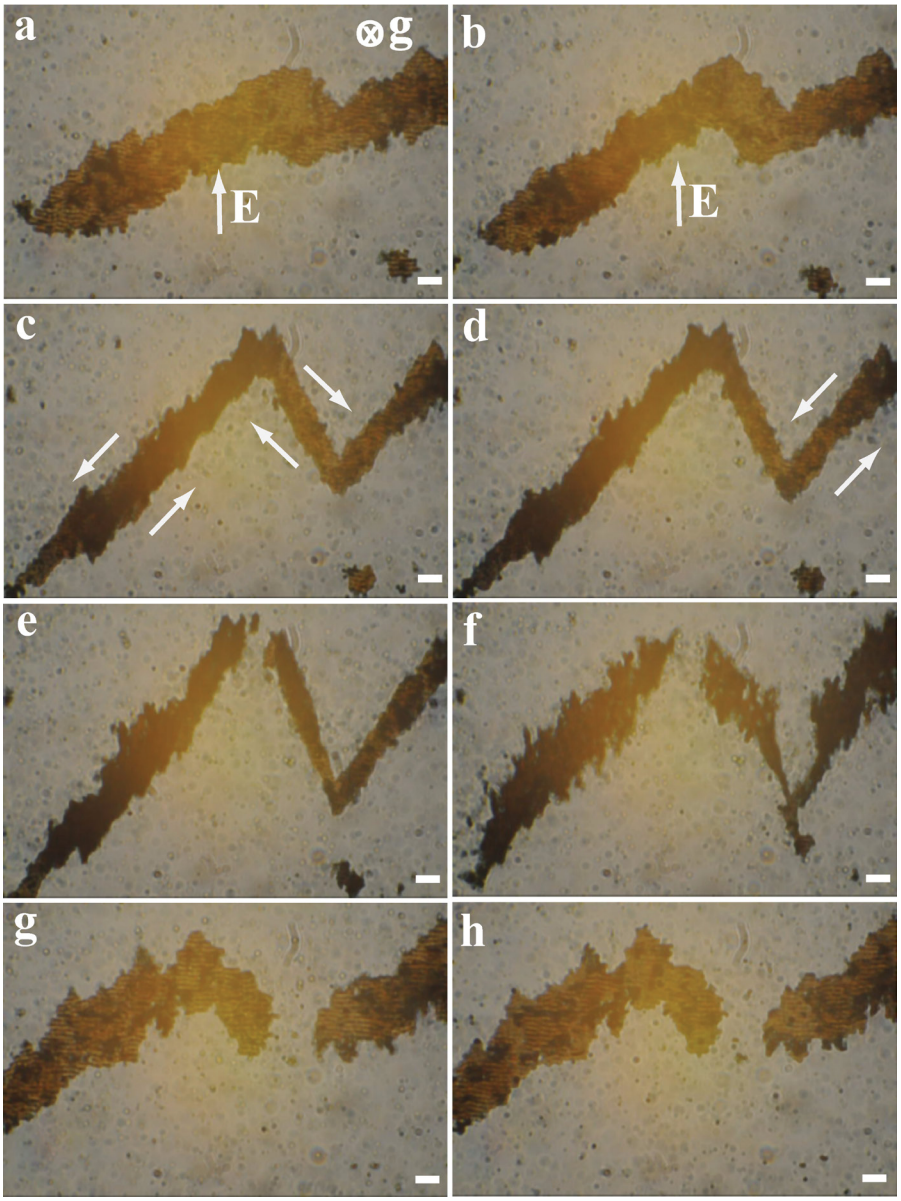

Figure S5. Electrohydrodynamic instability. (a-f) Optical micrographs showing the formation of diagonal bands that consist of stacks of columns when the field was increased to $E_{rms} \geq 0.04$ Vμm^{-1}, $f = 200$ kHz. (a) The directions of the applied electric field and gravity are indicated. (c-d) Arrows indicate the direction of the circulation. The time lapse between the frames is 30 secs. The field was turned off after 2-3 mins. As a result of strong circulations smaller columns resulted. (g-h) These columns were then exposed to a field of 0.015 Vμm^{-1}, which was below the critical field strength for onset of instabilities. Scale bars are 15 μm.

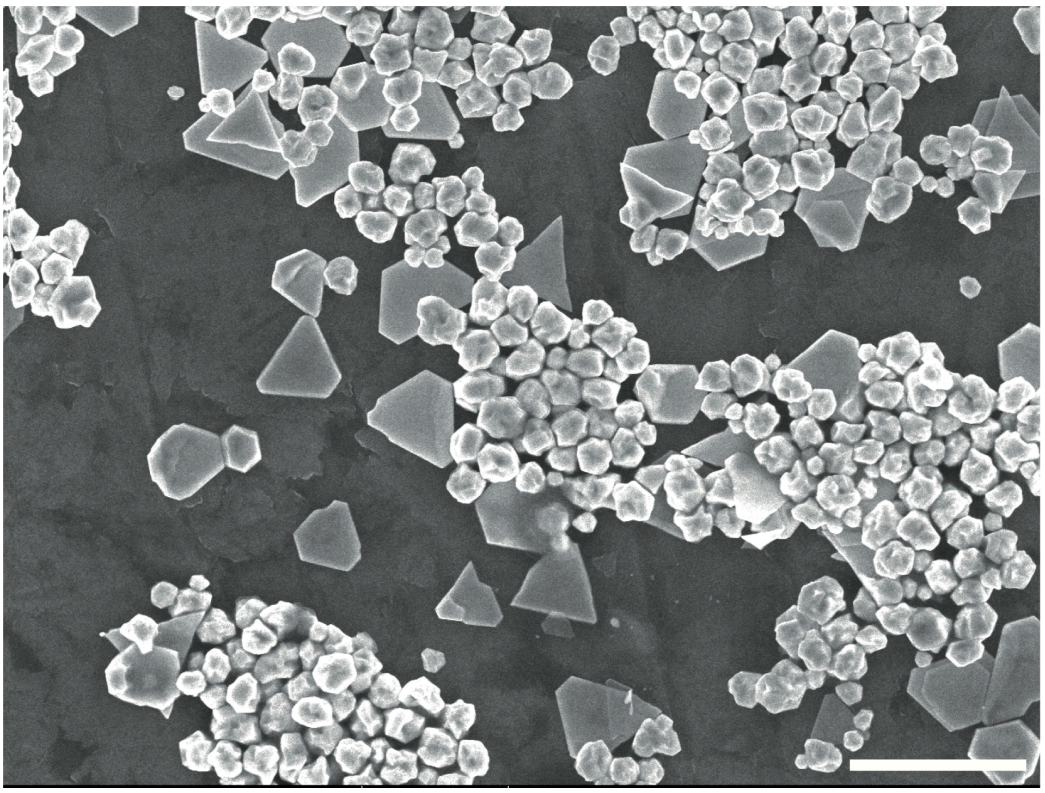

Figure S6. Thin gold platelets were synthesized by the Hachisu et al. method.[8] Scanning electron micrograph of typical synthesis. Scale bar is 2 μm.

Supplementary references:

(1) Verwey, E. J. W. *J. Phys. Colloid Chem.* **1947**, 51, 631-636.

(2) Derjaguin, B.; Landau, L. *Prog. Surf. Sci.* **1993**, 43, 30-59.

(3) Parsegian, V. A., *Van der Waals forces: a handbook for biologists, chemists, engineers, and physicists*. Cambridge University Press: 2005.

(4) Derjaguin, B. *Acta Physicochim. USSR* **1941**, 14, 633-662.

(5) Palik, E. D., *Handbook of optical constants of solids*. Academic press: 1998; Vol. 3.

(6) Hu, Y.; Glass, J. L.; Griffith, A. E.; Fraden, S. *J. Chem. Phys.* **1994**, 100, 4674-4682.

(7) Isambert, H.; Ajdari, A.; Viovy, J. L.; Prost, J. *Phys. Rev. Lett.* **1997**, 78, 971-974.

(8) Okamoto, S.; Hachisu, S. *J. Colloid and Inter. Sci.* **1973**, 43, 30-35.